frontiers | Frontiers in Physics

REVIEW
published: 29 April 2022
doi: 10.3389/fphy.2022.893791

A Review on Metamaterial Absorbers: Microwave to Optical

*Yadgar I. Abdulkarim[1,2], Ayesha Mohanty[3], Om Prakash Acharya[3], Bhargav Appasani[3], Mohammad S. Khan[4], S. K. Mohapatra[3], Fahmi F. Muhammadsharif[5] and Jian Dong[1]**

[1]School of Computer Science and Engineering, Central South University, Changsha, China, [2]Medical Physics Department, College of Medicals & Applied Science, Charmo University, Chamchamal, Sulaimania, Iraq, [3]School of Electronics Engineering, KIIT University, Bhubaneswar, India, [4]Department of Computer and Information Sciences, East Tennessee State University, Johnson City, TN, United States, [5]Department of Physics, Faculty of Science and Health, Koya University, Koya, Iraq

Metamaterials (MM) are artificially designed materials that possess unique properties due to their geometrical design. They also display some peculiar properties, such as negative refractive index, Snell's law reversal, Doppler effect reverse, and left-handed behavior. MMs are used in a myriad of applications, including invisibility cloaking, perfect lensing, perfect absorption, and sensing. In this review article, the property of electromagnetic absorption by structures known as metamaterial absorbers (MMAs) is discussed. An MMA is a composite made up of many layers of metallic patterns separated by dielectric. This novel device helps in achieving near-unity absorption by various mechanisms, which are investigated in this article. The MMAs are classified based on their absorption characteristics, such as polarization tunability, broadband operation, and multiband absorption, in different frequency regimes.

Keywords: metamaterials, left-handed materials, metamaterial based perfect absorbers, design of metamaterial absorbers, negative refraction

OPEN ACCESS

Edited by:
Petra Granitzer,
University of Graz, Austria

Reviewed by:
Parikshit Moitra,
University of Maryland, Baltimore, United States
Kebin Fan,
Nanjing University, China

****Correspondence:***
Jian Dong
dongjian@csu.edu.cn

Specialty section:
This article was submitted to Optics and Photonics, a section of the journal Frontiers in Physics

Received: *10 March 2022*
Accepted: *06 April 2022*
Published: *29 April 2022*

Citation:
Abdulkarim YI, Mohanty A, Acharya OP, Appasani B, Khan MS, Mohapatra SK, Muhammadsharif FF and Dong J (2022) A Review on Metamaterial Absorbers: Microwave to Optical. Front. Phys. 10:893791. doi: 10.3389/fphy.2022.893791

INTRODUCTION

We are living in a world that thrives off communication and exchange of information. However, the recent evolution of communication seriously provokes electromagnetic (EM) interference and contaminates the surrounding environment with EM pollution. Subsequently, the quality of humans is tempered by the typical behavior of devices. As a result, there is an increasing demand for the development of appropriate materials and procedures to mitigate the effects of EM waves. This demand has been fulfilled by the introduction of an absorber into the world of communication [1, 2].

An absorber is a block of material that is used to absorb some of the energy of an incident particle. Due to their potential applications in high efficiency solar cells, sensors and stealth technology, researches on absorbers are quickly increasing. Among the many valuable applications, the most common is military purposes or stealth technology. The goal of stealth technology is to conceal a jet from radar by covering it with materials that absorb radar signals. The absorber used in this technology can lower or block radar signals that reflect off the surface of an airplane. Some classical examples of EM absorbers include Dallenbach, Salisbury and Jaumann absorbers [3–6]. Nevertheless, the drawbacks of these conventional absorbers are owed to their thick size and design complexity, making them unsuitable for many practical applications [7, 8]. Therefore, the research focus moved towards the metamaterial absorbers (MMA) in order to meet the need for compact and simple absorbers. Metamaterial-based absorbers (MMAs) have received much attention due to their high absorption, thin layers

and low density. MMAs can trap or absorb an incident EM wave in some specific points of the device then eventually convert the EM into heat.

Metamaterial (MM), defined by Walser in 2001 [9], is a combination of two terms, "meta" and "material," which refers to a material having properties sublime to the conventional material. MMs can be comprised of three-dimensional or two-dimensional periodically designed macroscopic composites that display exotic properties extending from microwave to optical frequencies. The properties unavailable in conventional materials include the inverse Doppler effect, negative refractive index, perfect lensing, left-handed behavior, electromagnetic wave cloaking, and perfect absorption [10–13]. Out of all the unnatural properties, metamaterial-based absorbers (MMAs) offer perfect absorption, thus making them highly efficient to capture solar energy and to be used with sensors, bolometers, wireless power transfer, and perfect light absorber. The first metamaterial absorber was suggested by Landy et al. [14], which had merits of thin thickness and compact size in comparison with the conventional absorbers. Numerous works on the optimized absorbers have been proposed since then. The MMA can be designed with multiband, broadband, polarization, and tunablility characteristics for different applications such as solar cell, sensors, and thermal imaging. For over a decade, various metamaterial absorbers from microwave to optical frequency regimes have been produced, and a number of novel applications have been reported [15–20]. However, combining a multiband MMA with high efficiency is still not easy, and sensitive absorption conditions can be broken easily. A closer look at the literature reveals that some issues remain to be explored along with a systematic approach to design an optimum metamaterial-based absorber. The issues associated with the design of MMA are increasing the number of absorption bands, improving the working conditions, polarization tunable absorbers, material selection parameter, among other practical usages.

Many researchers have become fascinated by the absorbance achieved using metamaterials in recent years. This absorbance is due to the controllable and tunable effects arising from the alternation of the coupling between the patches in the MM structure at a resonance frequency of the electromagnetic wave. In this review, numerous works on metamaterial absorbers, including the absorption mechanisms, have been investigated. The manipulation of polarization characteristics in the MMA allows switchable absorption in different frequencies. Similarly, by controlling the distance or gaps between the coupling components, multiband absorption can be obtained. Again, variation in the shape of the patches helps to yield near-perfect absorption. Moreover, near-unity absorption is feasible by varying the parameters of MMA along with the dielectric thickness, unit cell period, and material selection.

This review is conceived in different sections, providing a generalized idea about the metamaterial absorbers operating in different frequency regimes.

Genesis of Metamaterials

The existence of metamaterials was first envisioned by Victor Veselago [21], a Russian physicist, in his seminal research paper on the existence of materials with negative refractive index. He described their characteristics decades before their physical realization. This section describes the theoretical background of metamaterials, which begins with Maxwell's laws on electromagnetism [22]. For an electromagnetic (EM) time-harmonic wave propagating in a lossy medium with conductivity "σ," permittivity "ε" and permeability "μ," four laws are given in differential form by **Eqs 1–4**:

$$\nabla.E_s = 0 \tag{1}$$

$$\nabla.H_s = 0 \tag{2}$$

$$\nabla\times E_s = -j\omega\mu H_s \tag{3}$$

$$\nabla\times H_s = (\sigma + j\omega\varepsilon)E_s \tag{4}$$

Applying curls on both the sides of **Eq. 3**, we get the electric field for the waves in a lossy dielectric:

$$\nabla^2 E_s - \gamma^2 E_s = 0 \tag{5}$$

where $\gamma = \sqrt{j\omega\mu(\sigma + j\omega\varepsilon)}$, which is known as the propagation constant.

Similarly, the magnetic field can be possibly written as:

$$\nabla^2 H_s - \gamma^2 H_s = 0 \tag{6}$$

Eqs 5, **6** are known as the Helmholtz equations, or wave equations.

If the wave is a plane monochromatic wave travelling in the z direction, the electric and magnetic fields propagate in the x and y directions, respectively. The previous equations can be simplified further. Then, the electric field could be expressed as:

$$E_s = E_x(z)a_x \tag{7}$$

Substituting **Eq. 7** with **Eq. 5**, the solution of the wave equation becomes:

$$E_x(z) = E_0 e^{\gamma z} + E_0^{'} e^{-\gamma z} \tag{8}$$

Then, the electric field vector can be expressed by:

$$E(z,t) = Real\left(E_x(z)a_x e^{j\omega t}\right) \tag{9}$$

As γ is a complex number, it can be represented as $\gamma = \alpha + j\beta$. Thus, the above equation becomes:

$$E(z,t) = E_0 e^{-\alpha z}\cos(\omega t - kz)a_x \tag{10}$$

Similarly, the magnetic field in the y direction is given by:

$$H(z,t) = H_0 e^{-\alpha z}\cos(\omega t - kz)a_y \tag{11}$$

The relation between E_0 and H_0 can be obtained from **Eq. 4**:

$$H_0 = E_0/\eta \tag{12}$$

where η is the characteristic or intrinsic impedance of the medium.

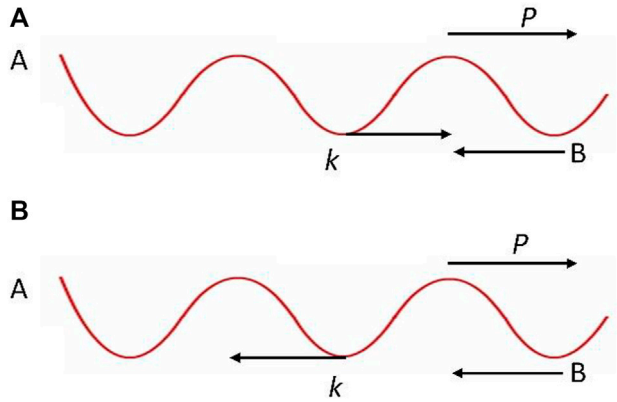

FIGURE 1 | Wave propagation in **(A)** RHM and **(B)** LHM.

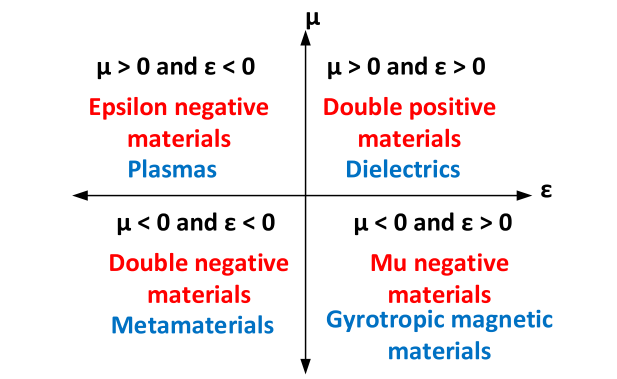

FIGURE 2 | Classification of materials.

If the medium is lossless, then $\sigma \cong 0$, and, thus the E-field and H-field are in phase with one another, $\alpha = 0$, $k = \omega\sqrt{\mu\varepsilon}$:

$$|\eta| = \sqrt{\mu/\varepsilon} \tag{13}$$

Therefore, the velocity of the wave becomes:

$$v = \frac{1}{\sqrt{\mu\varepsilon}} \tag{14}$$

The permittivity (ε) and permeability (μ) of a medium affect the propagation of the electromagnetic wave. In media with these two parameters, the direction of wave propagation with A and B as the respective source and receiver obeys the right-hand rule, i.e., the wave vector k and the Poynting vector p are in the same direction, and called right-handed materials. Interestingly, these two parameters also tend to be negative. The wave propagation in the media is opposite to that in the right-handed materials (RHM), i.e., p and k are in opposite directions, as shown in **Figure 1**. These are known as left-handed materials (LHM) [23–29].

Thus, the parameters ε and μ characterizes the propagation of the wave in a medium. The materials are divided into four categories based on their permittivity and permeability characteristics, which are specified in **Figure 2**.

The first group of material are named double positive (DPS) material, as both ε and μ of the material are greater than zero. This category primarily contains dielectrics. Permittivity is less than zero and permeability is larger than zero in the second category, which is why it is termed epsilon negative (ENG) material. Many plasmas exhibit these properties at certain frequency regimes. The third group materials possess a permittivity greater than zero and permeability less than zero. Gyro tropic magnetic materials display these characteristics and are called mu negative (MNG) material. The fourth group contains the double negative (DNG) material, which can only be produced artificially. This class of material has both permittivity and permeability less than zero, or negative. When an EM wave enters such media, the direction of wave propagation reverses. No naturally available material has both negative permeability and permittivity. From the above classification, metamaterials can be defined as a special class of materials that are artificially designed to display negative permittivity and negative permeability [30–34]. However, with the continuous design and development of more structures with unique properties and applications, a broader definition is used to classify them as metamaterials. The metamaterial is a man-made macroscopic composite designed with a periodic cellular architecture to produce a complex interaction with electromagnetic waves to achieve the desired performance, which cannot be obtained using naturally available material [35–39].

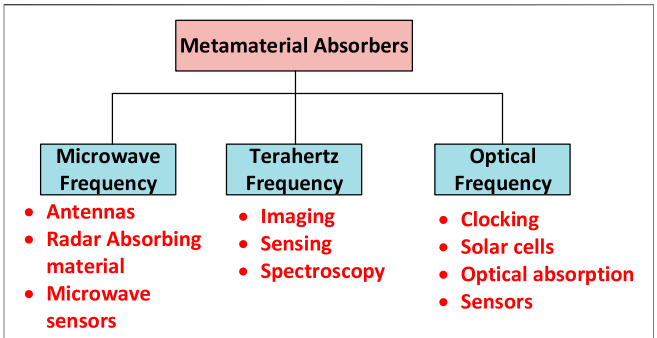

FIGURE 3 | Applications of metamaterial absorber with respect to different frequencies.

Metamaterial Absorber

MMA is a block of material used to absorb some of the energy of an incident particle and is usually comprised of three layers. MMAs are also called a perfect absorber with near-unity absorption, showing zero reflection and transmission coefficients for plane waves that are typically incident. However, multi-layer absorbers are also designed to provide broadband characteristics. The metallic pattern is the first layer, which is arranged periodically. The second layer consists of a substrate or dielectric layer. Finally, the third layer is another periodic metallic pattern.

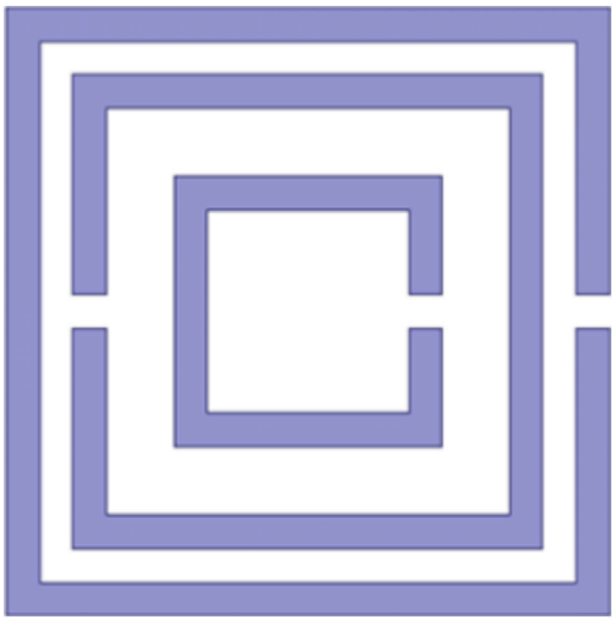

FIGURE 4 | Split ring resonator.

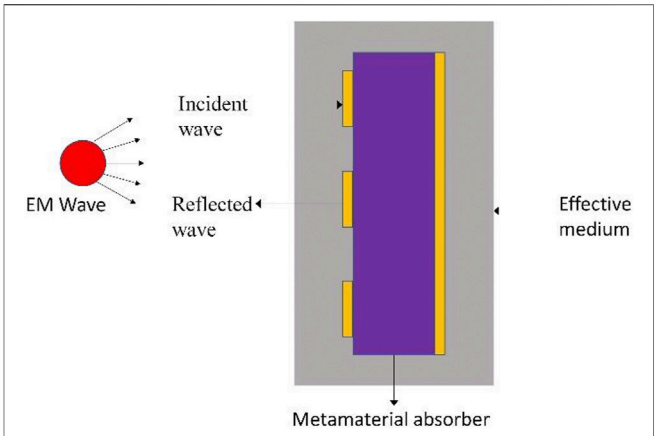

FIGURE 5 | Impedance matching in a metamaterial absorber.

Active manipulation of EM wave propagation results in achieving one of the interesting characteristics in metamaterials, which is absorption. This phenomenon occurs when electromagnetic radiation or light is absorbed after encountering such material. The reason behind this manipulation is the generation of absorption property by adjusting ε and μ values. Metamaterial absorbers are being designed for RF frequency applications, extending from microwaves to optical frequency, such as sensors, photodetectors, solar cells, and emitters [40]. MMAs are classified into three different frequencies and applications based on that is demonstrated in **Figure 3**.

ABSORPTION MECHANISM

The absorption characteristics displayed by these structures are attributed to the negative values of ε and μ, impedance matching, reduction in plasma frequency of metals, strong electric and magnetic resonances, etc. These factors are manipulated by the proper choice of the absorber's geometrical configuration. A detailed discussion of three absorption mechanisms is given in the following subsections.

Magnetic and Electrical Resonances

The absorption mechanism of perfect absorbers relies on electric and magnetic resonances. Magnetic resonances can be achieved using closed loop-like structures, whereas electrical resonances can be achieved by creating gaps in the structures. Proper structural design may be used to tune both the electric and magnetic characteristics. One of the most common types of resonators is the split ring resonator (SRR) which is the widely-adopted absorber designs that utilizes the principle of magnetic and electrical resonances for achieving absorption characteristics, as shown in **Figure 4**. In fact, the first metamaterial absorber designed by Landy and his colleagues is based on the same principle. Concentric SRRs are usually adopted for achieving multiband absorption characteristics [41–46]The mutual coupling between these absorbers produces additional absorption bands, and closely spaced concentric SRRs results in wideband absorption characteristics.

Impedance Matching

The next principle that may be responsible for EM absorption is the matching of impedance. This is a well-known phenomenon that occurs when electromagnetic waves travel from one medium to another, whereby some EM energy gets reflected and the remaining energy gets transmitted. Reflection is minimized when the characteristic impedance of the reflected medium matches that of the incident medium, as shown in **Figure 5**. To achieve optimum performance in an absorber design, impedance matching is a challenging task. As in most cases, the first medium happens to be air with a characteristic impedance is around 377 Ω; therefore, the impedance of the absorber should be near to this value at the desired frequency in order to achieve near unity absorption [47–50].

Reduction in Plasma Frequency

The plasma frequency of a material is the frequency at which the density of the electron gas oscillates and is given by:

$$\omega_p = \sqrt{\frac{Ne^2}{m\varepsilon_0}}\omega_p \tag{15}$$

where,

ω_p—Plasma frequency
N—Density of the free electron gas
m—Effective mass
e—charge of an electron

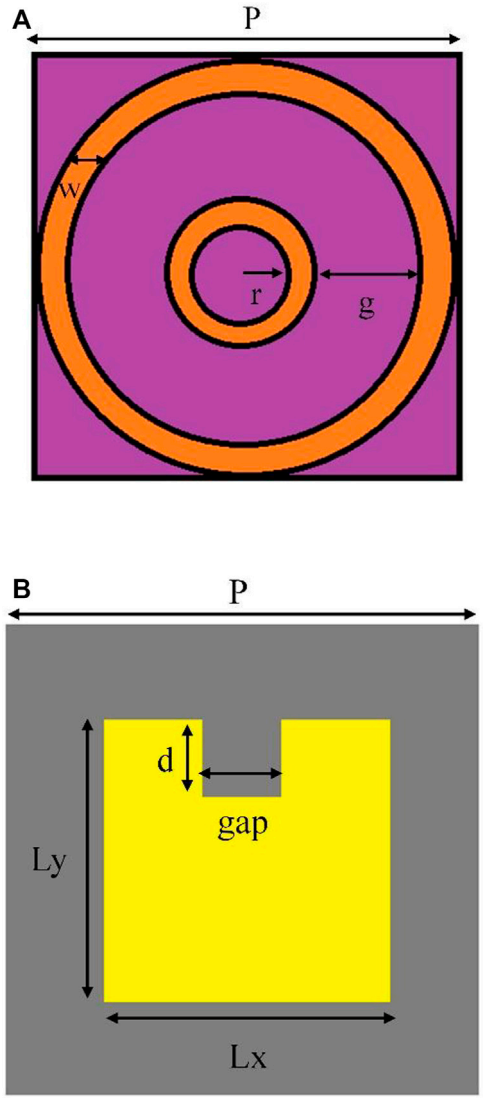

FIGURE 6 | Metamaterial perfect absorbers **(A)** ring and **(B)** patch.

From **Eq. 15**, it is clear that the plasma frequency ω_p totally depends on the density of the free electron carriers of the metal. In the case of semiconductors, plasma frequency can be increased or decreased by doping the medium. Materials with negative permittivity can be formed by reducing the plasma frequency, which is based on the operating frequency of the metamaterial absorber. The main reason for the reduction in plasma frequency is to fabricate MM absorbers that can operate in various frequency regimes. Therefore, it is highly pertinent to set the frequency according to the targeted frequency regime [51–53].

DESIGNS OF METAMATERIAL ABSORBERS

As mentioned, MMAs are three-layered structures containing a top metallic plane, middle dielectric layer, and a bottom ground plane. The widely-adopted designs of these perfect absorbers are given in **Figure 6**.

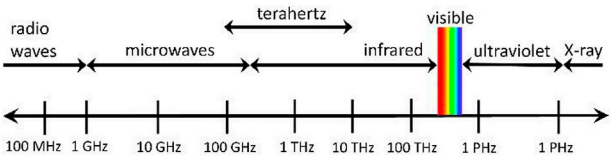

FIGURE 7 | Electromagnetic spectrum.

Metamaterial absorbers are predominantly used in the microwave, terahertz, and optical frequency spectra based on their requirements in various applications.

The electromagnetic spectrum from 100 MHz to 1 PHz is depicted in **Figure 7**.

Microwave Frequency

MMAs for microwave frequencies are mostly designed for X-band applications, including radar and other surveillance applications where electromagnetic shielding has practical utility. Thus, much of the research is directed towards designing absorbers in this frequency range. In 2008, Landy et al. [14] designed the most prominent and first-ever narrowband metamaterial absorber using split ring resonator (SRR) and a cut wire. As illustrated in **Figure 8**, the design comprised of three layers: two conducting resonators and a dielectric substrate.

In **Figure 8**, the metamaterial designed by [14] achieved a 96% narrowband absorption spectrum at 11.48 GHz by simulation and 88% spectrum at 11.5 GHz *via* experimentation. The first reported MMA offered narrowband absorption owing to the magnetic coupling between the split ring and cut wire in the parallel plane. The magnetic response was achieved by the antiparallel currents due to the cut wire and centre wire of the resonators. The absorption mechanism was theoretically explained by Ohmic and dielectric losses, as elaborated in **Figure 8E**.

Subsequent efforts were made to increase the absorption bandwidth of the MMA. Specifically, researchers heavily focused on designing multiband, broadband and frequency tunable metamaterial absorbers [55–58]. Initially, MMAs with multiband absorption characteristics were developed using multiple resonant unit cells, then merging the cells through a co-planar arrangement [59–62].

Park et al. [59] implemented a donut structure multiband absorber at microwave frequencies and validated its performance through simulation and experiment. As shown in **Figure 9**, the unit cell of this design was made up of a metallic layer with four different patterns on top and a ground plane on the bottom. Multiple absorption bands generated by antiparallel surface currents between the front and rear plates were caused by magnetic resonance in the top metallic layer. The MMA design also exhibited polarization insensitivity, whereby the multiband absorption spectrum was not affected by the change in polarization angles and incidence angles. This effect was

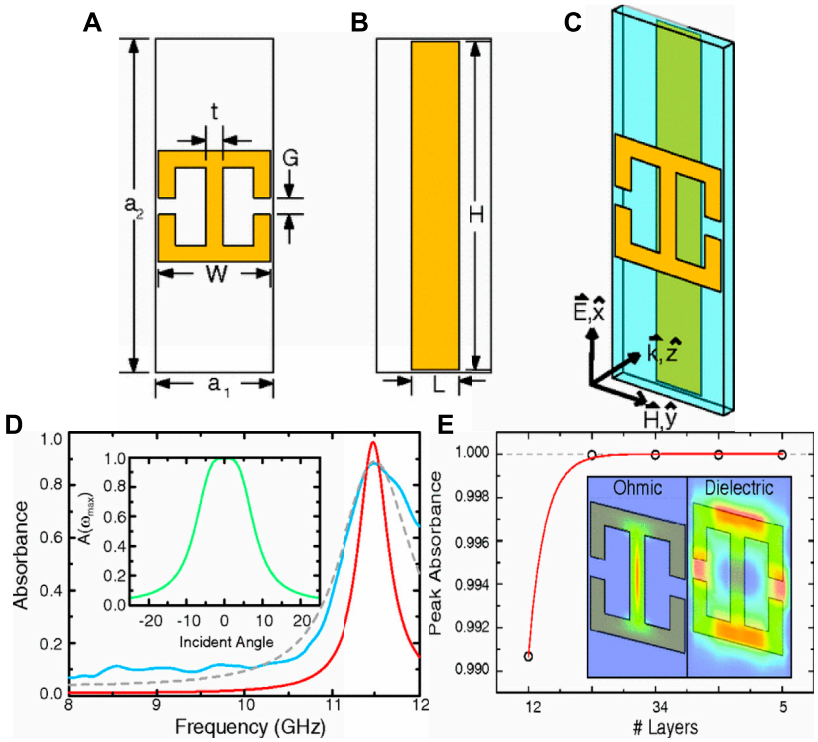

FIGURE 8 | (A) Schematic absorber structure, **(B)** cut wire, **(C)** unit cell displaying the direction of wave propagation. **(D)** Absorption spectra with respect to frequency and incident angle. **(E)** Simulated A(ω) with increasing MM layers; Insets show the simulated losses at resonance: Ohmic loss (surface) is shown in the left inset panel, and the dielectric (volume) loss is on the right. Adapted with permission from Ref. [14]. Copyright (2008) American Physical Society.

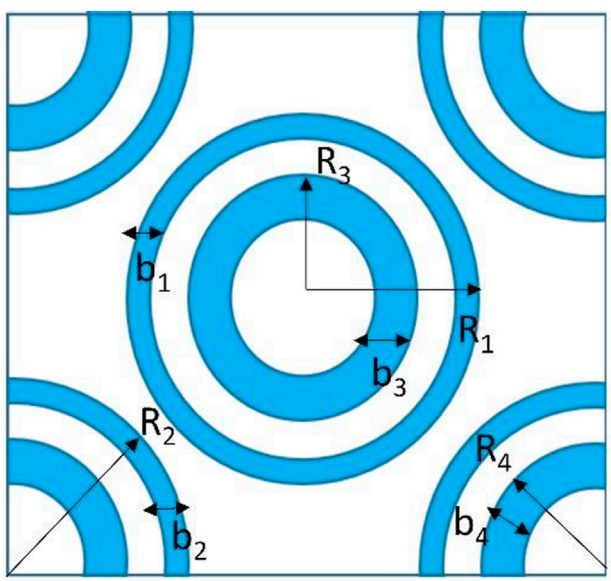

FIGURE 9 | Schematic of the MMA.

because of the symmetrical absorber structure. The metamaterial perfect absorber achieved absorption of 97%, 97%, 98%, and 98% at 6.5, 7.4, 9.2, and 11.0 GHz, respectively, using FR-4 as the dielectric substrate.

Similarly, Zheng et al. [60] proposed a dual-band perfect absorber by combining Fabry-Perot cavity resonance and optical-transmission effect. Two separate structures, consisting of a copper layer and FR-4 dielectric substrate were prepared for the unit cell design. Changes in the distance of these two structures resulted in the absorption spectra for this MMA. Particularly, the absorption bands decreased as the distance decreased, and the absorption spectra reduced from dual band to single band.

In the microwave region, Ghosh et al. [61] proposed a metamaterial absorber made up of an array of linked rings. A split ring and a full ring were included in each pair of rings. The absorption characteristic of the absorber was given by its equivalent RLC circuit model, whereby the maximum absorption was caused by impedance matching. Dual narrowband absorption was formed due to the multiple sets of rings. Parametric analysis was used to illustrate the design geometry decision by analysing various incidence and polarisation angles. Finally, the design was fabricated for the practical applications. Taking the whole structure, absorption peaks of 96% and 92.5% occurred at 9.66 and 10.26 GHz, respectively. Moreover, Wang et al. [62] developed a quad-band MMA, obtaining four absorption bands with the peaks of 99.47%, 99.94%, 99.05%, and 99.55% at 28.21, 39.59, 52.78, and 58.63 GHz, respectively. The connection between the ring resonators was attributed for the absorption characteristics.

By changing the dimensions of an MMA and shape of the metallic patch, such as a symmetric structure, numerous absorption bands can be achieved. Apart from the design of multiband MMAs, researchers have started to work on broadband MMAs. A broadband response signifies that a device is able to absorb all electromagnetic frequencies illuminating from the MMA surface. In order to broaden the bandwidth, multi-layer stacked structures and multiple metallic metamaterial structures have been proposed in the literature [51–59]. Planar and vertical arrangement approaches are other names for these design ideas. Numerous metallic patterns on the top layer of the planar arrangement enhance the near frequency of multiple resonances, allowing for broadband absorption with excellent absorptivity. Multiple top layers are stacked vertically in the vertical arrangement, resulting in broadband absorption. Tunability is another important characteristic of MMAs. Tunable absorbers are those that can be tuned by varying some parameters, such as frequency, polarization angles, incidence angles, dimension of the absorber layer, etc. By implementing an asymmetric patch structure, near-perfect absorptivity can also be achieved by tunable MMAs.

In 2012, Lee et al. [63] designed a broadband metamaterial-based near-perfect I-shaped absorber in microwave frequencies that gave both narrowband and broadband absorption. The narrowband peak was due to the multi-layered model with an absorption greater than 99.5% at 13.5 GHz, while the broadband absorption, which was dependent on the resonance frequency, was created by the length of the cut-wire bar. Based on the simulated and measured absorption spectra. It was discovered that as the cut-wire length is reduced, the electric resonance frequency increases. This perfect absorber can be efficiently applied in military radar devices.

M. C. Tran et al. [116] constructed, simulated, and tested a broadband metamaterial microwave absorber. Unlike the standard technique, which relies solely on unit cell boundary conditions, they used full-sized setups to do full-wave finite integration simulations. This study incorporates the digital notion of coding metamaterials into the metamaterial absorber system. Coding and digital metamaterials are a relatively recent topic of study that has garnered a lot of interest. In this paper, four types of coding metamaterial blocks, 2×2, 3×3, 4×4, and 6×6 blocks, were optimized and then employed as building blocks (meta-block) for the development of various 12×12 topologies with a realistic size scale, starting from a basic unit cell structure. The broadband absorption response was discovered in the frequency range 16–33 GHz, and it was shown to be in good agreement with the analogous medium theory prediction and experimental observation.

The Internet of Things (IoT) is expected to become completely ubiquitous in the future. To realise this vision, a new generation of IoT devices that can operate independently must be developed. IoT devices must be totally wireless in terms of transmission and power in order to gain autonomy. Accurate sensing is also an important aspect of autonomy. Several wireless standards have been established to help IoT applications run more efficiently.

Electromagnetic waves can now be used as a source of energy, as well as a carrier for exchanging data, thanks to the development of metamaterial perfect absorbers (MPAs). Sensors are an important component of IoT technology that uses a lot of power in low-power IoT devices. Nonetheless, the energy generated by EM energy harvesting may be sufficient to run most existing low-power sensors used in a variety of industries, including medical, food, and agricultural.

So, M. Amiri et al. [117] investigated various metamaterial absorbers applicable to IoT. In this review, authors have conducted extensive research on the present applications from MMA which are beneficial such as energy harvesting, optical switching and sensing. The best thing which they have mentioned in this review is the feasible directions for implementation of MMA in industrial applications.

Similarly, Bakir et al. [58] presented an absorber that can operate in the microwave regime and is useful in sensing applications, including pressure, temperature, density, and humidity sensors. A unit cell design composed of a circular split ring and square ring resonators was created by the authors. The square and ring resonators were made of copper metal, and DiClad 5.27 was used as the dielectric material. The design was verified both experimentally and numerically as metamaterial absorber and it was used for sensor application, displaying both narrowband and broadband absorption characteristics. A copper plate was placed behind the dielectric substrate to support the resonators for the absorber specification, and a sensor layer was placed behind the resonators in place of the copper plates for the sensor specification. The incident wave from free space impedance matching and the intrinsic impedance of the MMA are used in the design, which is based on absorption characteristics.

In many military applications, such as radar cross section (RCS) reduction, cloaking devices, and sensor detectors, perfect absorbers are highly desirable. However, most techniques (such as wedge and pyramidal absorbers, multi-resonant absorbers) have concerns with low-frequency size, bandwidth, and absorption ratio. So, Wang et al. [139] solved these problems by merging Huygens metasurface and the three-layers slab impedance metasurface. The former meets the innovative impedance matching theory, while the latter has multi-resonant qualities and optimised conductivities, resulting in high-efficiency absorption at lower frequencies (1–3 GHz) and higher frequencies (3–18 GHz). Authors designed, demonstrated and fabricated a realistic microwave metasurface absorber and conducted experiments to show that it can reach ultra-broadband (118 GHz) performance with an absorption rate more than 75%. The numerical calculations correspond well with the results, showing that by refining the designs, it can boost the absorption efficiency to 92% throughout the whole working band. Their discoveries have the potential to accelerate the development of ultra-broadband meta-devices, notably cloaking technologies based on high-efficiency absorption.

Ding et al. [64] also realized an ultra-broadband polarization-independent metamaterial absorber in the microwave range. The authors designed an absorber consisting of multi-layered quadrangular frustum pyramids, where the unit cell structure was made up of 20 metallic patches in shape of a pyramid. The absorption process was owing to the metal layers overlapping.

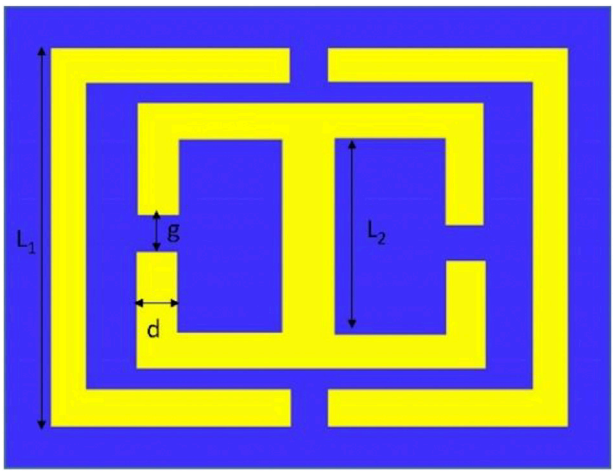

FIGURE 10 | Simulated unit cell structure.

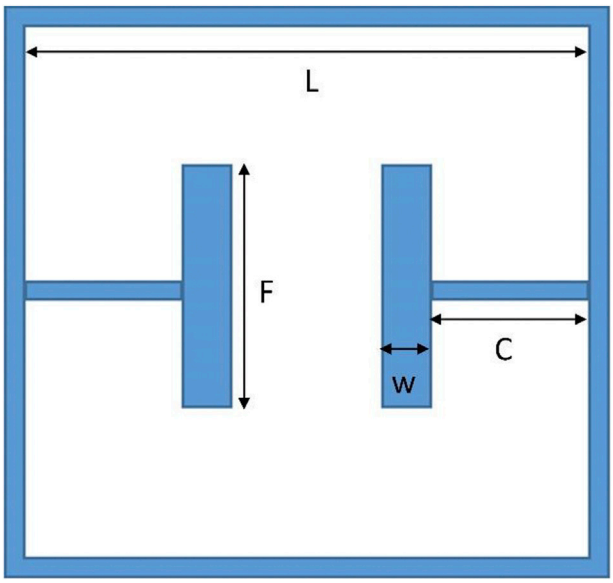

FIGURE 11 | Schematic of the MMA.

The design was validated by measuring the absorption spectra experimental findings to the modelling results.

Ozden et al. [65] developed a new MM-based broadband RF absorber operating at the X-band frequency, which is critical in stealth technology. The proposed structure is comprised of two concentric rings placed on a dielectric spacer, as shown in **Figure 10**. The dielectric layer was composed of epoxy glass cloth laminate (FR4) material, and copper material was chosen for metallic rings as well as the ground plane. The designed absorber was simulated and measured in the X-band (8–12 GHz) range and was simulated for 12- and 16-unit cells separately. The planar absorber achieved the highest absorption level of 80% at X-band with bandwidths of 2.73 and 2.55 GHz for 12 unit cells and 16 unit cells, respectively. As seen in the simulation, an absorption of 97.95% and 98.40% was achieved by the absorber structure. The absorption mechanism for broadband operation was investigated by electric and magnetic field strength plots.

Ling and others proposed a novel frequency tunable metamaterial absorber [66], which was the first MMA to be made with natural cork. The novel tuning mechanism was influenced by the topology of the absorber and the properties of the substrate. The structure consisted of an SRR pattern, as shown in **Figure 11**, which was designed on cork sheets having good hygroscopicity. The suggested absorber's absorption ratio is simulated and measured in varied moisture content (M = 0%, 1.44%, 5.88%, 13.32%, and 18.8%) of the cork substrate in this study. The resonance frequency varied from 4.92 GHz in the dry (M = 0%) state to 3.49 GHz in the wet (M = 18.8%) state, with observed absorptivity more than 90% throughout all moisture content levels.

This specific absorber may be used to develop wireless humidity sensors since the frequency of the absorber can be adjusted by altering the moisture. Similarly, more works related to microwave frequency are given in **Table 1**.

Furthermore, our focus moves towards the performance of metamaterial absorbers as sensors on the basis of their absorption characteristics. So, the comparison of performance related to the unit cell size, substrate material and application can be seen in **Table 2**.

Terahertz Frequency

The terahertz frequency domain, which ranges from 1 to 10 THz, is located between microwave and infrared (IR) frequencies. THz MMAs have recently piqued researchers' interest owing to their potential applications in imaging and spectroscopy, the non-ionizing nature of THz rays, and their ability to permeate materials such as plastics, paper, and fabric. Although these absorbers were initially designed for the microwave frequency range due to simple fabrication, but they eventually became more popular for realization over a wide spectrum range. Now, these absorbers can be designed by varying the geometrical dimensions operating in a spectrum ranging from THz to visible frequencies. The flexibility of the structural design is a promising feature that allows researchers to fill the THz gap. In the last decade, many THz MMAs have been realized theoretically and experimentally implemented in thin metallic wires, fishnet [67–69], SRRs [70–72], U-shaped resonators [73, 74], chiral structures [75] and graphene-based MMAs [76–83]. They also exhibit large potential in the terahertz regime. Therefore, this section presents the progress of THz metamaterial absorbers [84–91].

Yen et al. [43] experimentally developed the first terahertz frequency absorber in 2004. The structure was created utilizing a planar layer of double SRR array suitable for terahertz devices. The absorber's mechanism was based on a basic resonator construction. The magnetic response was about 1 THz due to the interaction between the two split rings. Considering the magnetic resonant behavior in THz frequency, the dimensions of SRRs have been scaled down by analytical methods and numerical simulation.

TABLE 1 | Metamaterial absorbers in Microwave Range.

Ref. No	Absorption type	Polarization Insensitivity	Angle Insensitivity	Frequency Range
[118]	Broadband	Yes	Yes	X (8–12 GHz) Ku (12–18 GHz) bands
[119]	Broadband	Yes	Yes	1–8 GHz
[120]	Multiband	N/A	N/A	8–12 GHz (X-band)
[121]	Ultra-wideband	Yes	Yes	8–12 GHz (X-band)

TABLE 2 | Performance Comparison of Metamaterial absorbers based Sensors in Microwave Range.

Ref. No	Unit Cell Size (mm)	Substrate material	Operating frequency (GHz)	Application
[141]	36 × 36	FR-4	2–6	Permittivity sensor
[142]	40 × 20	F4B	<1	Permittivity sensor
[143]	28 × 35	FR-4	3–5	Micro-fluid sensor
[144]	24 × 30	FR-4	3–6	Temperature sensor

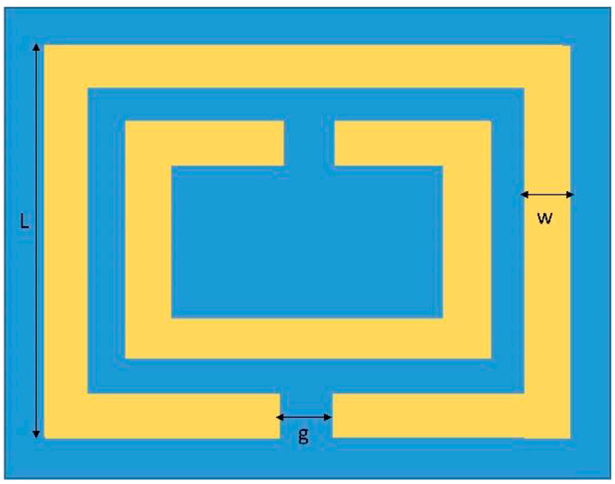

FIGURE 12 | Schematic of double SRR.

Subsequently, Tao et al. [92] experimentally demonstrated a metamaterial design at terahertz frequencies illustrated in **Figure 12**. The structure was made up of an array of SRRs, where the top metallic layer consisted of SRRs and the bottom metallic layer was designed for driving of currents that circulate between the two layers. This circulating current was generated from an incident magnetic field. The absorption peaks were attributed to the LC resonance and high order dipole resonance in this study, with the inductance provided by the two loops on either side of the central capacitor. Experimentally, an absorption of 0.96 at 1.6 THz was obtained from the absorber structure.

Researchers have further explored multiband THz MMAs. For instance, Wang et al. [93] demonstrated a metamaterial absorber design with dual band absorption property, consisting of a U-shaped metallic patch. Gold was selected as the material for the top metallic patch and ground plane. The absorber showed dual band absorption characteristics with peaks at 1.80 and 2.97 THz, and absorption of more than 98% was due to the LC resonance overlapping and dipole response of the metallic framework.

Shan et al. [94] presented a flexible dual band ultrathin absorber that can be applied in micro-bolometers and stealth aircraft. The structure of the absorber consisted of split ring resonators with uneven gaps. The metallic rings and the ground plane were made of aluminum, and the dielectric layer was prepared with polyimide. The simulated absorption plot reveals 99.7 and 99.6% absorptions at 0.41 and 0.75 THz frequency, respectively, which is attributed to normal dipole resonances and high order dipole resonance.

Wang et al. [95] implemented an asymmetric metallic cross terahertz absorber for sensing application. The 3-layered structure is comprised of a gold metallic cross and ground plane separated by a dielectric spacer. The design achieved absorption peaks of 99.07% at 1.23 THz, 99.84% at 2.39 THz, and 99.01% at 3.19 THz. The authors also found the absorption mechanism to be totally dependent on the fundamental resonances, whereby the strong magnetic resonances gave rise to the triple absorption peaks with near-unity absorption.

Wang et al. [96] further designed a novel quad-band terahertz absorber based on a U-shaped resonator, yielding near-unity absorption. The structure gave four modes of resonance bands at frequencies of 0.33, 0.99, 1.73, and 1.93 THz. In this metamaterial absorber, the two metal layers were made up of gold. The authors designed a simpler structure that was easy to fabricate, and the absorption mechanism was elaborately investigated by the electric field distribution of four modes of resonance. The peaks are due to the LC resonance, dipole resonance, quadrupedal resonance, and localized response or high order response of the resonator. This perfect metamaterial absorber can be applied in the fields of material detection, thermal imaging, and biological sensing.

Mohanty et al. [97] presented a multiband terahertz metamaterial absorber comprised of a Π- and U-shaped structure. A schematic of the asymmetric metamaterial absorber displaying the top view is shown in **Figure 13**. For the structural design, the authors chose aluminum as the metallic layer and polyimide as the dielectric substrate. The absorption

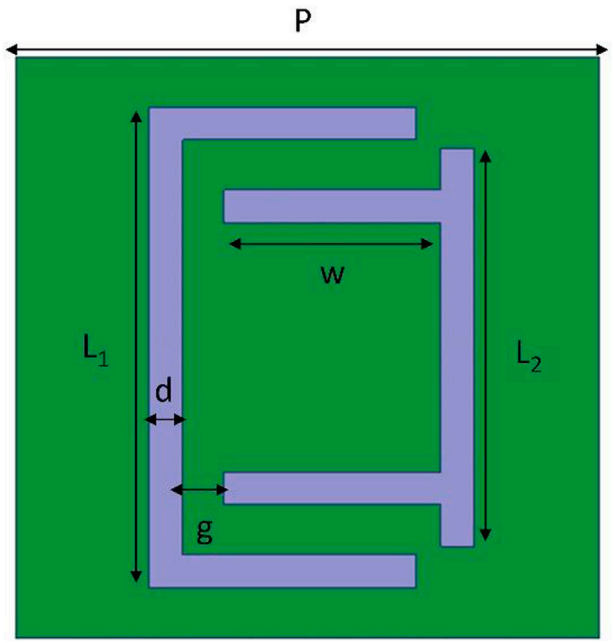

FIGURE 13 | Schematic of a metamaterial-based perfect absorber.

characteristics of the model were owed to the electromagnetic coupling of the top metallic patch structure. The simulation results revealed that three prominent absorption peaks with an average absorption of 97% were achieved by the proposed metamaterial structure with respective absorptivity of 97.78%, 97.92% and 96.81% at frequencies of 1.45, 1.80, and 2.70 THz. Moreover, parametric analysis was performed by evaluating different dielectric thicknesses, periods of the unit cell, incidence angles, and polarization angles. Furthermore, the absorption mechanism was explained by the electric filed strength plots at resonant frequencies, demonstrating that this MMA can be utilized in terahertz spectroscopy and imaging.

Wen et al. [98] introduced 2 THz devices using metamaterial based perfect absorbers and modulators that are highly desirable for various applications, such as stealth technology, thermal emitters, detector, and phase imaging. High speed modulators and perfect absorbers are the key components of the communication system. In this work, the authors experimentally demonstrated a broadband absorber consisting of a periodic array of aluminum squares of two different dimensions. The absorber structure gave rise to an absorption bandwidth of over 200 GHz with absorption magnitude of 90%. From the results, it was found that the silicon dioxide dielectric layer significantly improved the design. Subsequently, the authors proposed a metamaterial-based THz modulator made up of VO_2 cut-wires, which was fabricated by magnetron sputtering and conventional lithographic technologies.

Broadband THz MMAs have also been designed and reported in the literature. For example, He et al. [45] created a broadband terahertz absorber on a metal sheet using an array of graphene-dielectric multi-layered frustum pyramids. Hyperbolic dispersion and anisotropic permittivity are found in this graphene-based MMA. Surface plasmonic waves impacting on the graphene layers are absorbed at different levels of the pyramid in this pyramid construction. The absorption of the waves can be attributed to the squeezing effect of the slow waves. The numerical simulation results indicate that high absorption was achieved with a bandwidth from 8 THz to over 100 THz and that the floquet periodic mode contributed to the wave absorption. This graphene-based absorber has applications in THz detectors and thermal emitters. Similarly, Zhu et al. [99] demonstrated a metamaterial absorber operating at terahertz frequencies *via* simulation and experiment. The design includes an array of truncated pyramid unit structure made up of five layers of metal film. *Via* numerical simulation, both the TE and TM polarization were examined. The results show that at normal incidence, more than 80% absorption was achieved in the range of 0.75–1.5 THz and ultra-wide band absorption was seen for different incidence angles. Experimentally, five layers of the pyramid structure contributed absorptivity of more than 80% for each layer. Finally, the authors compared simulation and measured results of a single layer, which were well-matched at resonance frequency 0.8 THz. The wide-angle absorber showed to be polarization insensitive and have practical application by easy integration with semiconductor technology. Li et al. [100] numerically demonstrated an ultra-broadband MMA, which was investigated by optimizing the structural parameters. By merging the resonance peaks of the terahertz planar metamaterial absorber, a broadband absorption spectrum was produced. Parametric analysis was conducted by varying the polarization angles and incidence angles, concluding that the absorption does not depend on the polarization angles. Hence, the presented MMA was polarization insensitive. Pan et al. [132] proposed a broadband MMA made up of two circular gold split rings and a polyimide dielectric spacer. The absorption mechanism was studied on the basis of energy distribution of the three resonant peaks, which were because of strong electric and magnetic resonances in the absorber. The broadband width was attributed to the overlapping of the three resonances. Considering the symmetric design of the absorber, the structure displayed the same curve for both modes (TE and TM). Terahertz spectrum imaging, detection, and stealthy technology are some of the applications of this absorber.

From the presented works, it can be inferred that the metamaterial absorbers displaying broadband or wideband absorption are usually made up of multiple layers or stacked layers and multiple top metallic patches. The addition of multiple layers using different dielectrics and metals helps to yield broadband absorption. Similarly, the multiple top metallic patterns placed near proximity to one another in each unit cell can superpose with each other to achieve perfect broadband absorption. Other important THz MMAs are summarized in **Table 3**.

Apart from these narrowband and broadband MMA structure, the most recent metamaterial absorber which has got all the attention is the MMA for biomedical sensing applications. Although there are variety of applications involving metamaterials, the MMA having potential sensing application

TABLE 3 | Metamaterial absorbers in terahertz range.

Ref. No	Absorption type	Polarization Insensitivity	Angle Insensitivity	Frequency Range
[122]	Multiband	Yes	Yes	0.4–1.1
[123]	Multiband	N/A	N/A	0–2
[124]	Four-band	Yes	Yes	0.5–2.5
[125]	Narrow band	N/A	N/A	0.2–2
[36]	Single, Dual, Broad band	N/A	N/A	1–3
[126]	Triple-band	N/A	N/A	0–2.5
[127]	Dual-band	N/A	N/A	20–30
[128]	Quadband	Yes	N/A	1–4.2
[74]	Six band	N/A	N/A	0–4
[129]	Five band	N/A	N/A	0.5–3.5
[130]	Narrow band	Yes	Yes	4–7
[131]	Ultra-broad band	Yes	Yes	1–3
[91]	Broadband	Yes	Yes	2.6–3.5

in biomedical field has given rise to a lot of research work during the pandemic.

Saadeldin et al. [133] proposed a unique design of perfect metamaterial absorber for terahertz sensing applications. At the resonance frequency, the proposed structure worked by increasing the confinement of both electric and magnetic fields at the same time. As a result, at 2.249 THz, an absorptivity of 0.99 is reached with a narrow resonant peak and a Q-factor of 22.05. At constant analyte thickness, the resonance frequency is sensitive to the surrounding medium refractive index. As a result, the presented metamaterial design can be employed as a refractive index (RI) sensor with a high sensitivity of 300 GHz/RIU and a figure of merit (FoM) of 2.94 over a refractive index (RI) range of 1.0–1.39 at a thickness of 1 μm. Authors also mentioned one important biomedical application in their work. As most of the biological samples refractive index ranges from 1.3 to 1.39, the MMA structure is simulated with a given analyte RI of 1.35. The MMA based refractive index sensor exhibited a sensitivity of 23.7 GHz/μm for the detection of sensing layer thickness fluctuation. So, the structure can be utilized for future biological applications as it has a high sensitivity.

Similarly, Hou et al. [135] demonstrated a terahertz MM based biosensor with polarization insensitive characteristics for bovine serum albumin detection. Because of its inherent superiority, terahertz (THz) metamaterials are frequently employed in biosensor devices, and the need for novel high sensitivity biosensors based on THz metamaterials is growing. In this work, when the sensor is coated with analytes of varied refractive index and thickness, the peak of the transmission spectrum moves dramatically, according to simulation. The sensor's sensitivity may reach 135 GHz/RIU after being coated with 10 m thick non-destructive analytes. Experiments reveal that the lowest detectable concentration of BSA solutions by this sensor is 0.1 mg/ml, and that when the concentration is 17.6 mg/ml, the transmission spectrum's peak red shift reaches 137 GHz, with a frequency shift percentage of 16.4 percent. This research offered a very sensitive biosensor detecting approach for the pharmaceutical and food industries.

Mohanty et al. [136] proposed a terahertz metamaterial absorber for sensing applications. Authors have used finite element method for analyzing the refractive index (RI) sensor based on MMA. Due to the ensuing impact of coupling between the two identical patches, the MMA provided a significant resonant peak with near 100% absorbance at frequency 4.5 THz. Surface current distribution, absorption mechanism, and structural parametric analysis were also looked at. The peak is designated as A, with a line width of 0.02 THz and a quality factor (Q-factor) of 225, which is sensitive to the refractive index of the environment (RI) shown in **Figure 15**. As a result of its very sensitive sensing capabilities, the innovative design may be employed as a refractive index sensor, with a sensitivity of 1.6 THz per refractive index unit (RIU) and a figure of merit (FoM) of 80 in terms of change in RI of the surrounding environment. As stated earlier in Ref. [133], majority of blood samples are in the RI range of 1.3–1.39. So, this novel design along with the similar work in Ref. [137] might be helpful in future practical biomedical applications.

Hassan et al. [138] investigated biosensing platforms for virus detection based on metamaterial and plasmonic. New infections for humans are continually emerging as a result of changes in our environment and the ongoing loss of habitat for animals. The SARS-CoV-2 virus has grown so contagious and lethal that it has posed a new challenge to healthcare's technological growth. Humans have been exposed to numerous additional deadly viral epidemics in the last decade, including Zika virus, Ebola virus, MERS-coronavirus, and others, and there may be even more contagious and deadly viruses on the future. Though traditional methods have been successful in detecting these infections to some extent, they are time-consuming, expensive, and need highly skilled human resources. Biosensors based on plasmonic metamaterials might open the way for low-cost, quick viral detection. The authors presented the latest developments in plasmonic and metamaterial-based plasmonic biosensors for the detection of viruses and viral particles.

Jing et al. [140] demonstrated a stainless-steel terahertz metamaterial absorber. This absorber is made up of all-metal metamaterial layers and substrate layers, with the metamaterial layer's geometric form being a ring. The research establishes the theoretical feasibility as well as enhanced sensing capabilities. The absorber achieves a 99.95% narrow peak absorption at 1.563 THz, according to simulation data. Geometric characteristics can be

TABLE 4 | Comparison between the sensing performances of the existing absorbers.

Ref. No	Q-Factor	FoM	Refractive Index Range (*n*)	Resolution (RIU)
[145]	7	0.5	1.0–4.0	1
[146]	15	3	1.0–2.0	0.2
[147]	7	1.5	1.0–2.0	0.2
[148]	41	2.3	1.0–2.0	0.2
[149]	58	7.5	1.0–1.6	0.2
[136]	225	80	1.0–1.36	0.01
[133]	22.1	2.94	1.35–1.39	0.01

used to adjust the absorption. This remarkable absorption efficiency was made possible by the ring metamaterial layer's electric and magnetic resonances. The resonance frequency of the absorber varies significantly depending on the refractive index, and the sensor's sensitivity is 74.18 μm/RIU with a Q-factor of 36.35. Furthermore, the absorber used in this work is stainless steel and does not have a sandwiched structure. The stainless-steel material is less expensive and easier to produce, allowing it to be used in a variety of applications. Their findings might be useful in optoelectronic devices, biosensors, and optical switching.

Hence, a detailed comparison table showing the Q-factor, FoM and refractive index range of some more metamaterial absorber based sensors is shown in **Table 4**.

Optical Frequency

The optical MMAs are a type of perfect absorbers operating in optical frequency or mid-infrared (mid-IR) frequency, specifically 300–430 THz. The main constraint for designing perfect absorbers in the optical region is the size of the unit cell. The unit cell dimension must be in nanometers, which can be realized practically using nano-fabrication techniques. Hence, optical or mid IR metamaterial-based absorbers have fascinated researchers due to their efficient application in electromagnetic cloaking and solar cells [45, 101–104].

Avitzour et al. [106] made the first attempt of designing a metamaterial-based perfect absorber operating in the IR region. Though the structure was complex, it still offered more than 90% of absorption with near-zero reflectivity. The authors claimed that using a double layer contributes to the absorption level of nearly 99%. In 2010, Hao et al. [107] realized an ultrathin wide-angle metamaterial absorber for the optical frequency regime. The simple metallic nanostructures were comprised of gold film as the metallic layer and using Al_2O_3 as the dielectric spacer, through which near perfect absorption was achieved. By verifying the performance of this absorber, the structure was found to be angle insensitive and also tunable. This tunable and angle insensitivity characteristic was achieved by adjusting the dimensions of the nanostructure. In the experimental setup, quartz substrate was chosen for the fabrication of multi-layered metamaterial absorber. A maximum absorption of 88% at wavelength of 1.58 μm was obtained experimentally and 97% by simulation. The difference in the absorption peaks was due to the fabrication tolerances.

Bossard et al. [108] presented a broadband polarization-insensitive optical metamaterial absorber with a super octave bandwidth. The authors reported that the absorber provided near-unity absorption. The generic algorithm was applied for the identification of the geometry of a single metallic screen supporting multiple overlapping. As illustrated in **Figure 14**, a superstrate layer was employed in the design for impedance matching, which resulted in the maximum absorption of the light. In this case, palladium (Pd) was employed as the metal to help broaden the bandwidth and improve the fabrication reproducibility.

In the wavelength range of 1.77–4.81 μm and in the 45° angular range, the electromagnetic bandgap (EBG)-based metamaterial absorber obtained an average wide-angle absorption of 98% as given in **Figure 15**.

Grant et al. [109] reported multi-spectral materials that included hybridization of optical plasmonic filters and metamaterial absorbers operating in the mid-infrared and terahertz regimes. The authors presented a single component with optically multiplexed visible, mid-IR, and terahertz radiations, which maximizes the spectral information density. The device was formed by hybridizing a plasmonic and metamaterial structure that was capable of simultaneous filtering and absorbing, which could filter 15 visible wavelengths and absorb in the mid-infrared and terahertz regions. The authors also claimed that their synthetic multi-spectral component can be integrated with CMOS technology.

Chen et al. [110] presented a MMA operating in the mid-infrared frequency regime. With a quality factor of 9, this novel MM absorber obtained a high absorption intensity of up to 77% at 7.87 μm. The cut-wire used in the design was found to be polarization-dependent. The experimental and modelling findings were nearly identical, indicating the absorber's promise in the fields of sensing and optics.

Yang et al. [45] proposed a high absorption metamaterial absorber operating in both optical and infrared frequency regimes. The design was based on an indium tin oxide (ITO) substrate because of its high absorptivity and reflectivity. In the infrared regime, the absorber became highly reflective, and at visible wavelengths, it was transparent. The authors claimed that this absorber has plasmon applications for infrared and can be used as transparent electrode materials in photo-voltaic applications. Three types of infrared metamaterial absorbers were studied in this work, all of which had substantial absorption at 10.6 μm but were transparent in the visible area. The simulation findings further reveal that the absorber was polarization-insensitive owing to the symmetric structural design and had a good absorption efficiency for TE and TM polarization at 10.6 μm. To further validate the design, both experimental and simulated results were in good accordance.

Desouky et al. [111] theoretically demonstrated a mid-IR omnidirectional super absorber composed of multi-layered N-doped silicon, also called a silicon hyperbolic metamaterial (HMM). It was subsequently combined with a sub-hole Si grating, which resulted in a single band absorption of up to 0.948. The authors stated that by altering the grating characteristics, their suggested structure could be adjustable from 4.5 to 11 μm. The

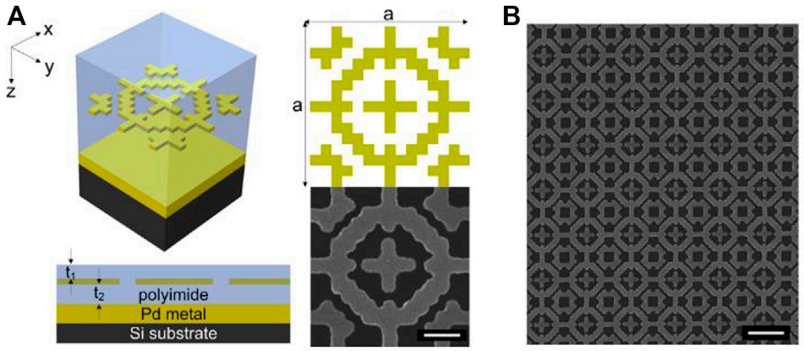

FIGURE 14 | (A) Schematic of the unit cell broadband absorber, **(B)** Nanofabricated image of the metamaterial absorber. Reprinted (adapted) with permission from [108]. Copyright (2014), American Chemical Society.

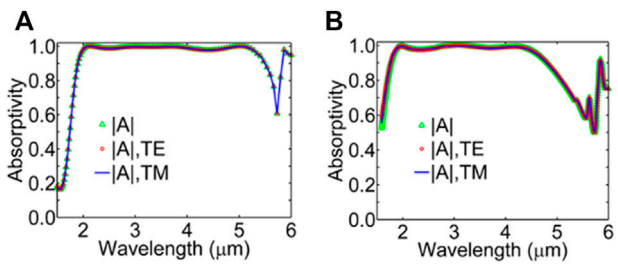

FIGURE 15 | (A) Simulated and **(B)** measured absorptivity of the design. Reprinted (adapted) with permission from [108]. Copyright (2014), American Chemical Society.

authors also created two grating structures using N-doped Si or Si HMM. The initial grating design was based on varying hole heights, with absorption ranging from 0.83 to 0.97 for wavelengths between 5 and 7 μm.

The second concept, which used different hole diameters to achieve a maximum broadband absorption of 0.97, was based on changing hole diameters. Considering these characteristics, the perfect absorber has efficient application in thermal energy harvesting.

Metamaterial absorbers made up of several tungsten cross resonators that function in the mid-infrared frequency band were introduced by Li et al. [104]. The structure exhibited near-unity absorption with a single absorption peak, which was achieved by tuning from 3.5 to 5.5 μm and adjusting the geometrical parameters. Then, different sizes of the multiple cross resonators were added in the one-unit cell. Broadband near-perfect absorption in the mid-infrared frequency range was achieved using this combination of two, three, or four resonators. From the absorption spectra, it was concluded that the metamaterial absorber exhibited omni-directionality and less dependency on incident polarization.

Ghaderi et al. [112] aimed to design and fabricate wideband CMOS compatible metamaterial absorbers operating in the mid-infrared region. The use of aluminum instead of another high conductivity metal ensured the CMOS compatibility. Masked UV lithography, instead of e-beam lithography, and CMOS-compatible fabrication were used for the design in the mid-IR frequency. The fabricated metamaterials showed a sensitivity towards the roughness of the surface. From the measurements, an absorption of 98% and the theoretical response were confirmed.

Dihan Hasan and Chengkuo Lee [113] presented a novel hybrid metamaterial platform in the mid-infrared frequency regime for optical sensing in the 5–8 μm spectral window. A CMOS-compatible metamaterial was combined with a gas trapping polymer to create the absorber. The results show that the sensor has a minimal detection rate of 40 ppm, a rapid reaction time, and low hysteresis. The smart polymer also enables multiplexed sensing, which may be utilized for gas concentration crosschecking and validation.

Ishii et al. [114] experimentally demonstrated spin current generation from plasmonic MM absorbers operating in the mid-infrared region. For creating a wavelength-selective spin current, the metamaterial absorbers were combined with platinum/yttrium-iron-garnet spintronic devices. Longitudinal spin seebeck effect (LSSE) and photo-spin-voltaic (PSV) effect were considered to be the origin of this spin current. The plasmonic resonance of the metamaterial absorber is responsible for the wavelength selectivity. Hence, the wavelength-selective IR sensor developed in this work can also be used in spin current generation.

P. Min et al. [115] presented an optically transparent flexible MMA. This proposed design exhibited broadband absorption characteristics by using topology optimization process based on generic algorithm (GA). A conformal optical transparent metamaterial absorber with broadband absorption extending from 5.3 to 15 GHz is developed, constructed, and measured to prove the method's effectiveness. The high agreement between experimental and numerical simulation findings further confirms the validity of their design and theoretical study. Both results show that the MMA has outstanding absorption properties, making it a popular choice for practical applications.

Lee et al. [134] presented a review on metamaterials (MM) and metasurfaces (MS) for sensor applications in optical

frequency. The authors investigated in detail about refractive index sensing with optical response and sensing properties of lights based on metamaterials and metasurfaces. In the realm of photonics, measuring variations in refractive index has been a popular and practical application. Refractive index sensor distinguishes itself by allowing for sensitive and label-free biochemical assays, enabling it to be used in a variety of chemical and biological sensing technologies. MM and MS based RI sensors are superior than traditional RI sensors in terms of manufacturing tolerance and readout signal stability because RI variation is monitored by macroscopic optical responses, primarily reflection or transmission of focused input beams. With fascinating physical phenomena such as plasmonically induced transparency and fano resonances, periodic configurations of MM permit reduced radiative damping and greater quality factor. With MM or MS, the functions of a single nanophotonic RI sensor might be expanded.

CONCLUSION AND FUTURE SCOPE

In this review work, the historical advancement of metamaterial-based absorber in various frequency bands (microwave to optical) is discussed in detail. Metamaterials are promising for producing absorbers and studying different exotic electromagnetic phenomena. Perfect absorption can be obtained from the suggested metamaterial absorbers with simple designs operating at lower or higher frequencies. These designs can be tweaked to show off additional features relevant to the intended practical uses. The most challenging aspect of the MMAs for GHz and lower frequencies is the size of the unit cell. Otherwise, flexible MMAs can be attained for microwave frequency by simple fabrication. However, this flexibility to work in different conditions and complex fabrication remain issues for absorbers operating in other higher frequencies. The optimized MMAs in the THz regime have potential application in the field of imaging and spectroscopy. In addition, higher fabrication tolerance is needed for the future application of MMAs in optical frequency. MMAs in the GHz and THz frequencies, like visible-range absorbers, require simpler designs, easier manufacturing, and lower production costs.

Increasing R&D actions for applications in defense, aerospace and telecommunication is a main goal driving the advancement of metamaterials. The demand and usage for metamaterial absorbers have rapidly in the past few years, considering their effective utilization in radar, vessels, and special smartphones. Presently, the metamaterial market is dominated by manufacturers using metamaterials for antenna and radar applications, such as Kymeta Corporation, JEM Engineering LLC, Metamaterial Technologies Inc., NKT Photonics AS, and Fractal Antenna Systems Inc. These are the major operational companies that are responsible for the rapid growth of metamaterials and the respective market. Recently, many developed countries have increased their national defence budgets, potentially leading to increased usage of metamaterial absorbers for defence applications. Considering the expansion of satellite communication, launching of more satellites will be required in the future to ensure smooth running and secured communication throughout the world. Essentially, this would also lead to increased utilization of metamaterials.

This review made a special effort to cover related articles on metamaterial absorbers in the microwave to optical frequency range, their historical advancement, and applications in diverse sectors. Nevertheless, some important contributions may have been missed, and the authors greatly apologize for the unintentional omission of other researchers' works.

AUTHOR CONTRIBUTIONS

AM and OA conceived the idea. YA, AM, OA, and BA wrote the manuscript. MK, SM and FM revised the manuscript. JD and BA supervise this work. All authors have read and agreed to the published version of the manuscript.

FUNDING

This work was supported by National Natural Science Foundation of China (Nos. 61801521 and 61971450); Natural Science Foundation of Hunan Province (No. 2018JJ2533); Fundamental Research Funds for the Central Universities (Nos. 2018gczd014 and 20190038020050).

REFERENCES

1. Bregar VB, Znidarsic A, Lisjak D, Drofenik M. Development and Characterisation of an Electromagnetic Absorber. *Materiali in Tehnologije* (2005) 39(3):89–93.
2. Li S, Qiao X, Chen J. Nano-Composite Electromagnetic Wave Absorbers [J]. *J Astronautics* (2006) 2.
3. Munk BA. *Frequency Selective Surfaces: Theory and Design*. John Wiley & Sons (2005).
4. Salisbury WW. *Absorbent Body for Electromagnetic Waves*. U.S.A: Google Patents (1952).
5. Ruck GT. *Radar Cross Section Handbook*, 2. Plenum Publishing Corporation (1970).
6. Chambers B, Tennant A. Active Dallenbach Radar Absorber. In: 2006 IEEE Antennas and Propagation Society International Symposium. IEEE (2006). p. 381–4.
7. Engheta N. *Metamaterials in Microwaves and Optics : A Review* (2006). p. 387–9.
8. Shamonina E, Solymar L. Metamaterials: How the Subject Started. *metamaterials* (2007) 11:12–8. doi:10.1016/j.metmat.2007.02.001
9. Walser RM. Electromagnetic Metamaterials. *Complex Mediums II: Beyond Linear Isotropic Dielectrics* (2001) 4467:1–15.
10. Shelby RA, Smith DR, Schultz S. Experimental Verification of a Negative Index of Refraction. *Science* (2001) 292(5514):77–9. doi:10.1126/science.1058847
11. Pendry JB. Negative Refraction Makes a Perfect Lens. *Phys Rev Lett* (2000) 85(18):3966–9. doi:10.1103/physrevlett.85.3966

12. Houck AA, Brock JB, Chuang IL. Experimental Observations of a Left-Handed Material that Obeys Snell's Law. *Phys Rev Lett* (2003) 90(13):137401. doi:10.1103/physrevlett.90.137401
13. Smith DR, Padilla WJ, Vier DC, Nemat-Nasser SC, Schultz S. Composite Medium with Simultaneously Negative Permeability and Permittivity. *Phys Rev Lett* (2000) 84(18):4184–7. doi:10.1103/physrevlett.84.4184
14. Landy NI, Sajuyigbe S, Mock JJ, Smith DR, Padilla WJ. Perfect Metamaterial Absorber. *Phys Rev Lett* (2008) 100(20):207402–1. –4. doi:10.1103/physrevlett.100.207402
15. Zhang W, Lan F, Xuan J, Mazumder P, Aghadjani M, Yang Z, et al. Ultrasensitive Dual-Band Terahertz Sensing with Metamaterial Perfect Absorber. *IEEE MTT-S Int Microwave Workshop Ser Adv Mater Process* (2017)(September) 1–3. doi:10.1109/imws-amp.2017.8247404
16. Bakshi SC, Mitra D, Minz L. A Compact Design of Multiband Terahertz Metamaterial Absorber with Frequency and Polarization Tunability. *Plasmonics* (2018) 13(6):1843–52. doi:10.1007/s11468-018-0698-2
17. Hedayati M, Faupel F, Elbahri M. Review of Plasmonic Nanocomposite Metamaterial Absorber. *Materials* (2014) 7:1221–48. doi:10.3390/ma7021221
18. Dubey A, Shami T. Metamaterials in Electromagnetic Wave Absorbers. *Dsj* (2012) 62(4):261–8. doi:10.14429/dsj.62.1514
19. Wang BX, Zhai X, Wang GZ, Huang WQ, Wang LL. A Novel Dual-Band Terahertz Metamaterial Absorber for a Sensor Application. *J Appl Phys* (2015) 117(1). doi:10.1063/1.4905261
20. Li D, Huang H, Xia H, Zeng J, Li H, Xie D. Temperature-dependent Tunable Terahertz Metamaterial Absorber for the Application of Light Modulator. *Results Phys* (2018) 11(October):659–64. doi:10.1016/j.rinp.2018.10.014
21. Veselago VG. The Electrodynamics of Substances with Simultaneously Negative Values of $\Epsilon$ and M. *Sov Phys Usp* (1968) 10(4):509–14. doi:10.1070/pu1968v010n04abeh003699
22. Kane Yee K. Numerical Solution of Initial Boundary Value Problems Involving maxwell's Equations in Isotropic media. *IEEE Trans Antennas Propagat* (1966) 14(3):302–7. doi:10.1109/tap.1966.1138693
23. Bilotti F, Pelosi G, Toscano A, Vegni L. From Artificial Engineered Materials to Metamaterials : 10 Th Anniversary of the Rome Workshops on ′ Metamaterials and Special Materials for Electromagnetic Applications and TLC. *7th Int Congress Adv Electromagn Mater Microwaves Opt – Metamaterials* (20132013)(September) 67–9.
24. Ramakrishna SA, Grzegorczyk TM. *Physics and Applications of Negative Refractive index Materials*. Bellingham, WA: CRC Press (2008).
25. Caloz C. Perspectives on EM Metamaterials. *Mater Today* (2009) 12(3): 12–20. doi:10.1016/s1369-7021(09)70071-9
26. Iyer AK, V Eleftheriades G. Negative Refractive index Metamaterials Supporting 2-D Waves. In: 2002 IEEE MTT-S International Microwave Symposium Digest (Cat. No. 02CH37278), 2 (2002). p. 1067–70.
27. Caloz C, Itoh T. Transmission Line Approach of Left-Handed (LH) Materials and Microstrip Implementation of an Artificial LH Transmission Line. *IEEE Trans Antennas Propagat* (2004) 52(5):1159–66. doi:10.1109/tap.2004.827249
28. Caloz C, Chang C-C, Itoh T. Full-wave Verification of the Fundamental Properties of Left-Handed Materials in Waveguide Configurations. *J Appl Phys* (2001) 90(11):5483–6. doi:10.1063/1.1408261
29. Lindell IV, Tretyakov SA, Nikoskinen KI, Ilvonen S. BW media?media with Negative Parameters, Capable of Supporting Backward Waves. *Microw Opt Technol Lett* (2001) 31(2):129–33. doi:10.1002/mop.1378
30. Ziolkowski RW, Heyman E. Wave Propagation in media Having Negative Permittivity and Permeability. *Phys Rev E* (2001) 64(5):56625. doi:10.1103/physreve.64.056625
31. Sun J, Liu L, Dong G, Zhou J. An Extremely Broad Band Metamaterial Absorber Based on Destructive Interference. *Opt Express* (2011) 19(22): 21155–62. doi:10.1364/oe.19.021155
32. Shen X, Cui TJ, Zhao J, Ma HF. *metamaterial absorber* (2011) 19(10): 20307–12. doi:10.1364/oe.19.009401
33. Engheta N, Ziolkowski RW. *Metamaterials: Physics and Engineering Explorations*. John Wiley & Sons (2006).
34. Marqués R, Medina F, Rafii-El-Idrissi R. Role of Bianisotropy in Negative Permeability and Left-Handed Metamaterials. *Phys Rev B* (2002) 65(14): 144440. doi:10.1103/physrevb.65.144440
35. Zhu B, Feng Y, Zhao J, Huang C, Wang Z, Jiang T. Polarization Modulation by Tunable Electromagnetic Metamaterial Reflector/absorber. *Opt Express* (2010) 18(22):23196–203. doi:10.1364/oe.18.023196
36. Wang B-X, Wang L-L, Wang G-Z, Huang W-Q, Li X-F, Zhai X. Frequency Continuous Tunable Terahertz Metamaterial Absorber. *J Lightwave Technol* (2014) 32(6):1183–9. doi:10.1109/jlt.2014.2300094
37. Wang B-X, Xie Q, Dong G, Huang W-Q. Design of Triple-Band Polarization Controlled Terahertz Metamaterial Absorber. *Superlattices and Microstructures* (2018) 114:225–32. doi:10.1016/j.spmi.2017.12.042
38. Bai N, Xiang W, Shen J, Shen C, Sun X. A Ka -Band Folded Waveguide Traveling Wave Tube with Lumped Resistance Metamaterial Absorber. *IEEE Trans Electron Devices* (2020) 67(3):1248–53. doi:10.1109/ted.2020.2967421
39. Tadesse AD, Acharya OP, Sahu S. Application of Metamaterials for Performance Enhancement of Planar Antennas: A Review. *Int J RF Microwave Computer-Aided Eng* (2020) 30(5):e22154. doi:10.1002/mmce.22154
40. Rhee JY, Yoo YJ, Kim KW, Kim YJ, Lee YP. Metamaterial-based Perfect Absorbers. *J Electromagn Waves Appl* (2014) 28(13):1541–80. doi:10.1080/09205071.2014.944273
41. Marqués R, Mesa F, Martel J, Medina F. Comparative Analysis of Edge- and Broadside-Coupled Split Ring Resonators for Metamaterial Design - Theory and Experiments. *IEEE Trans Antennas Propagat* (2003) 51(10):2572–81. doi:10.1109/tap.2003.817562
42. Chen H, Ran L, Huangfu J. Equivalent Circuit Model for Left-Handed Metamaterials Equivalent Circuit Model for Left-Handed Metamaterials. *J Appl Phys* (2006) 100:024915. doi:10.1063/1.2219986
43. Yen T, Padilla W, Fang N, Zhang X, Beijing T, "Terahertz Magnetic Response from Artificial Materials Terahertz Magnetic Response from Artificial Materials," *Science* no. 303(5663):1494–6. 2004. doi:10.1126/science.1094025
44. Baena JD, Marqués R, Medina F, Martel J. Artificial Magnetic Metamaterial Design by Using Spiral Resonators. *Phys Rev B* (2004) 69(1):14402. doi:10.1103/physrevb.69.014402
45. Yang J, Xu C, Qu S, Ma H, Wang J, Pang Y. Optical Transparent Infrared High Absorption Metamaterial Absorbers. *J Adv Dielect* (2018) 08(01): 1850007. doi:10.1142/s2010135x18500078
46. La Spada L, Vegni L. Metamaterial-based Wideband Electromagnetic Wave Absorber. *Opt Express* (2016) 24(6):5763. doi:10.1364/oe.24.005763
47. Matthaei GL, Young L, Jones EMT, and others, *Microwave Filters, Impedance-Matching Networks, and Coupling Structures*, vol. 5. McGraw-Hill New York, 1964.
48. Bahl IJ. *Lumped Elements for RF and Microwave Circuits*. Norwood, MA: Artech house (2003).
49. Gilbert E. Impedance Matching with Lossy Components. *IEEE Trans Circuits Syst* (1975) 22(2):96–100. doi:10.1109/tcs.1975.1084016
50. Sharma S, Tripathi CC, Rishi R. Impedance Matching Techniques for Microstrip Patch Antenna. *Indian J Sci Technol* (2017) 10(28):1–16. doi:10.17485/ijst/2017/v10i28/97642
51. Engheta N. Thin Absorbing Screens Using Metamaterial Surfaces. In: IEEE Antennas and Propagation Society International Symposium (IEEE Cat. No. 02CH37313), 2. IEEE (2002). p. 392–5.
52. Gang Q, Jia-Fu W, Ming-Bao Y, Wei C, Hong-Ya C, Yong-Feng L. Lowering Plasma Frequency by Enhancing the Effective Mass of Electrons: A Route to Deep Sub-wavelength Metamaterials. *Chin Phys B* (2013) 22(8):87302. doi:10.1088/1674-1056/22/8/087302
53. Hao J, Zhou L, Qiu M. Nearly Total Absorption of Light and Heat Generation by Plasmonic Metamaterials. *Phys Rev B* (2011) 83(16):165107. doi:10.1103/physrevb.83.165107
54. Wang B-X, Wang G-Z, Wang L-L. Design of a Novel Dual-Band Terahertz Metamaterial Absorber. *Plasmonics* (2016) 11(2):523–30. doi:10.1007/s11468-015-0076-2
55. Xin W, Binzhen Z, Wanjun W, Junlin W, Junping D. Design and Characterization of an Ultrabroadband Metamaterial Microwave Absorber. *IEEE Photon J.* (2017) 9(3):1–13. doi:10.1109/jphot.2017.2700056
56. Garg P, Jain P. Novel Ultrathin Penta-Band Metamaterial Absorber. *AEU - Int J Electron Commun* (2020) 116:153063. doi:10.1016/j.aeue.2020.153063
57. Dai X-W, Lin S-Y, Mao S-W, Luo GQ. Broadband Metamaterial Absorber with Double Resonant Modes Using Single-Layer Substrate. *AEU - Int J Electron Commun* (2020) 119:153179. doi:10.1016/j.aeue.2020.153179

58. Bakır M, Karaaslan M, Unal E, Akgol O, Sabah C. Microwave Metamaterial Absorber for Sensing Applications. *Opto-Electronics Rev* (2017) 25(4): 318–25.
59. Park JW, Van Tuong P, Rhee JY, Kim KW, Jang WH, Choi EH, et al. Multi-band Metamaterial Absorber Based on the Arrangement of Donut-type Resonators. *Opt Express* (2013) 21(8):9691–702. doi:10.1364/oe.21.009691
60. Zheng HY, Jin XR, Park JW, Lu YH, Rhee JY, Jang WH, et al. Tunable Dual-Band Perfect Absorbers Based on Extraordinary Optical Transmission and Fabry-Perot Cavity Resonance. *Opt Express* (2012) 20(21):24002–9. doi:10.1364/oe.20.024002
61. Ghosh S, Bhattacharyya S, Kaiprath Y. Bandwidth-enhanced Polarization-Insensitive Microwave Metamaterial Absorber and its Equivalent Circuit Model. *J Appl Phys* (2014) 115(10):104503. doi:10.1063/1.4868577
62. Wang N, Tong J, Zhou W, Jiang W, Li J, Dong X, et al. Novel Quadruple-Band Microwave Metamaterial Absorber. *IEEE Photon J* (2015) 7:1–6. doi:10.1109/jphot.2015.2399356
63. Lee YP, Tuong PV, Zheng HY, Rhee JY, Jang WH. An Application of Metamaterials: Perfect Absorbers. *J Korean Phys Soc* (2012) 60(8):1203–6. doi:10.3938/jkps.60.1203
64. Meng L, Zhao D, Li Q, Qiu M, 21. January (2013). p. 635–43. doi:10.1364/oe.21.00a229Polarization-sensitive Perfect Absorbers at Near-Infrared Wavelengths*Opt Express*
65. Ozden K, Yucedag OM, Kocer H. Metamaterial Based Broadband RF Absorber at X-Band. *AEU - Int J Electron Commun* (2016) 70(8):1062–70. doi:10.1016/j.aeue.2016.05.002
66. Ling K, Yoo M, Lim S, Lim S. Frequency Tunable Metamaterial Absorber Using Hygroscopicity of Nature Cork. *Antennas Wirel Propag Lett* (2015) 14: 1598–601. doi:10.1109/lawp.2015.2413939
67. Valentine J, Zhang S, Zentgraf T, Ulin-Avila E, Genov DA, Bartal G, et al. Three-dimensional Optical Metamaterial with a Negative Refractive index. *nature* (2008) 455(7211):376–9. doi:10.1038/nature07247
68. Zhou J, Koschny T, Kafesaki M, Soukoulis CM. Negative Refractive index Response of Weakly and Strongly Coupled Optical Metamaterials. *Phys Rev B* (2009) 80(3):35109. doi:10.1103/physrevb.80.035109
69. Guo H, Liu N, Fu L, Meyrath TP, Zentgraf T, Schweizer H, et al. Resonance Hybridization in Double Split-Ring Resonator Metamaterials. *Opt Express* (2007) 15(19):12095–101. doi:10.1364/oe.15.012095
70. Li D, Xie Y, Zhang J, Li J, Chen Z. Multilayer Filters with Split-Ring Resonator Metamaterials. *J Electromagn Waves Appl* (2008) 22(10):1420–9. doi:10.1163/156939308786348938
71. Shi C, Zang X-F, Wang Y, Chen L, Cai B, Zhu Y. A Polarization-independent Broadband Terahertz Absorber A Polarization-independent Broadband Terahertz Absorber. *Appl Phys Lett* (2014) 105:031104. doi:10.1063/1.4890617
72. Wang J, Qu S, Xu Z, Zhang J, Ma H, Yang Y, et al. Broadband Planar Left-Handed Metamaterials Using Split-Ring Resonator Pairs. *Photon Nanostructures - Fundamentals Appl* (2009) 7(2):108–13. doi:10.1016/j.photonics.2009.01.001
73. Li Z, Ma Y, Huang R, Singh R, Gu J, Tian Z, et al. Manipulating the Plasmon-Induced Transparency in Terahertz Metamaterials. *Opt Express* (2011) 19(9): 8912–9. doi:10.1364/oe.19.008912
74. Hu D, Wang H, Resonator C, "Design of Six-Band Terahertz Perfect Absorber Using a Simple U-Shaped Closed-Ring Resonator.," vol. 8, no. 2, p. 5500608. 2016.doi:10.1109/jphot.2016.2538758
75. Kenanakis G, Zhao R, Katsarakis N, Kafesaki M, Soukoulis CM, Economou EN. Optically Controllable THz Chiral Metamaterials. *Opt Express* (2014) 22(10):12149–59. doi:10.1364/oe.22.012149
76. Zhang H, Ling F, Wang H, Zhang Y, Zhang B. A Water Hybrid Graphene Metamaterial Absorber with Broadband Absorption. *Opt Commun* (2020) 463:125394. doi:10.1016/j.optcom.2020.125394
77. Qi Y, Zhang Y, Liu C, Zhang T, Zhang B, Wang L, et al. A Tunable Terahertz Metamaterial Absorber Composed of Elliptical Ring Graphene Arrays with Refractive index Sensing Application. *Results Phys* (2020) 16:103012. doi:10.1016/j.rinp.2020.103012
78. Cen C, Zhang Y, Chen X, Yang H, Yi Z, Yao W, et al. A Dual-Band Metamaterial Absorber for Graphene Surface Plasmon Resonance at Terahertz Frequency. *Physica E: Low-dimensional Syst Nanostructures* (2020) 117:113840. doi:10.1016/j.physe.2019.113840
79. Liu C, Qi L, Zhang X. Broadband Graphene-Based Metamaterial Absorbers. *AIP Adv* (2018) 8(1):15301. doi:10.1063/1.4998321
80. Patel SK, Charola S, Jani C, Ladumor M, Parmar J, Guo T. Graphene-based Highly Efficient and Broadband Solar Absorber. *Opt Mater* (2019) 96:109330. doi:10.1016/j.optmat.2019.109330
81. Mishra R, Sahu A, Panwar R. Cascaded Graphene Frequency Selective Surface Integrated Tunable Broadband Terahertz Metamaterial Absorber. *IEEE Photon J.* (2019) 11(2):1–10. doi:10.1109/jphot.2019.2900402
82. Zhang Y, Feng Y, Zhu B, Zhao J, Jiang T. Graphene Based Tunable Metamaterial Absorber and Polarization Modulation in Terahertz Frequency. *Opt Express* (2014) 22(19):22743. doi:10.1364/oe.22.022743
83. Hu B, Tao J, Zhang Y, Wang QJ. Magneto-plasmonics in Graphene-Dielectric sandwich. *Opt Express* (2014) 22(18):21727–38. doi:10.1364/oe.22.021727
84. Zhang Y, Wu P, Zhou Z, Chen X, Yi Z, Zhu J, et al. Study on Temperature Adjustable Terahertz Metamaterial Absorber Based on Vanadium Dioxide. *IEEE Access* (2020) 8:85154–61. doi:10.1109/access.2020.2992700
85. Wang B-X, Tang C, Niu Q, He Y, Zhu H, Huang W-Q. Broadband Terahertz Metamaterial Absorber Enabled by Using High-Loss Dielectric Materials. *Mater Res Express* (2019) 6(10):105804. doi:10.1088/2053-1591/ab422d
86. Guiming H. Design and Measure of a Tunable Double-Band Metamaterial Absorber in the THz Spectrum. *Mater Res Express* (2018) 5(4):45803. doi:10.1088/2053-1591/aabc00
87. Xiao D, Zhu M, Sun L, Zhao C, Wang Y, Tong Teo EH, et al. Flexible Ultra-wideband Terahertz Absorber Based on Vertically Aligned Carbon Nanotubes. *ACS Appl Mater Inter* (2019) 11(46):43671–80. doi:10.1021/acsami.9b14428
88. Xin B, Gui W, Wang Z. Temperature Tunable Metamaterial Absorber at THz Frequencies. *J Mater Sci Mater Electron* (2017) 28(12):8487–93. doi:10.1007/s10854-017-6570-x
89. Philip E, Zeki Güngördü M, Pal S, Kung P, Kim SM. Review on Polarization Selective Terahertz Metamaterials: from Chiral Metamaterials to Stereometamaterials. *J Infrared Milli Terahz Waves* (2017) 38(9):1047–66. doi:10.1007/s10762-017-0405-y
90. Wang A-X, Qu S-B, Yan M-b., Wang W-J, Wang J-f., Zheng L, et al. Six-band Polarization-Insensitive Perfect Metamaterial Absorber Using L-Shaped Resonators. *Appl Phys A* (2019) 125(5):331. doi:10.1007/s00339-019-2568-y
91. Mohanty A, Acharya OP, Appasani B, Mohapatra SK. A Broadband Polarization Insensitive Metamaterial Absorber Using Petal-Shaped Structure. *Plasmonics* (2020) 15(6):2147–52. doi:10.1007/s11468-020-01241-4
92. Tao H, Landy NI, Bingham CM, Zhang X, Averitt RD, Padilla WJ. A Metamaterial Absorber for the Terahertz Regime: Design, Fabrication and Characterization. *Opt Express* (2008) 16(10):7181–8. doi:10.1364/oe.16.007181
93. Wang B-X, Wang G-Z, Wang L-L. Design of a Novel Dual-Band Terahertz Metamaterial Absorber. *Plasmonics* (2016) 11(2):523–30. doi:10.1007/s11468-015-0076-2
94. Shan Y, Chen L, Shi C, Cheng Z, Zang X, Xu B, et al. Ultrathin Flexible Dual Band Terahertz Absorber. *Opt Commun* (2015) 350:63–70. doi:10.1016/j.optcom.2015.03.072
95. Wang B, Wang G, Sang T. Simple Design of Novel Triple-Band Terahertz Metamaterial Absorber for Sensing Application. *J Phys D: Appl Phys* (2016) 165307(49):1–7. doi:10.1088/0022-3727/49/16/165307
96. Wang B-X, Wang G-Z, Wang G, Wang B, Wang L, Wang G. Novel Quad-Band Terahertz Metamaterial Absorber Based on Single Pattern U-Shaped Resonator. *Appl Phys Express* (2017) 10:034301. doi:10.7567/apex.10.034301
97. Mohanty A, Acharya OP, Appasani B, Mohapatra SK. A Multi-Band Terahertz Metamaterial Absorber Based on a Π and U-Shaped Structure. *Photon Nanostructures - Fundamentals Appl* (2018) 32:74–80. doi:10.1016/j.photonics.2018.10.008
98. Wenp Q, Chent Z, Devices I, "Metamaterials Based Terahertz Absorber and Modulator," pp. 1–3. 2017. doi:10.1109/IMWS-AMP.2016.7588372
99. Zhu J, Ma Z, Sun W, Ding F, He Q, Zhou L, et al. Ultra-broadband Terahertz Metamaterial Absorber. *Appl Phys Lett* (2014) 105(2):10–4. doi:10.1063/1.4890521
100. Li X, Liu H, Sun Q, Huang N. Ultra-broadband and Polarization-Insensitive Wide-Angle Terahertz Metamaterial Absorber. *Photon Nanostructures - Fundamentals Appl* (2015) 15:81–8. doi:10.1016/j.photonics.2015.04.002

101. Liao YL, Zhao Y. Ultra-narrowband Dielectric Metamaterial Absorber with Ultra-sparse Nanowire Grids for Sensing Applications. *Sci Rep* (2020) 10(1): 1480–7. doi:10.1038/s41598-020-58456-y
102. Wang Y, Chen Z, Xu D, Yi Z, Chen X, Chen J, et al. Triple-band Perfect Metamaterial Absorber with Good Operating Angle Polarization Tolerance Based on Split Ring Arrays. *Results Phys* (2020) 16:102951. doi:10.1016/j.rinp.2020.102951
103. Qin F, Chen Z, Chen X, Yi Z, Yao W, Duan T, et al. A Tunable Triple-Band Near-Infrared Metamaterial Absorber Based on Au Nano-Cuboids Array. *Nanomaterials* (2020) 10(2):207. doi:10.3390/nano10020207
104. Li Z, Stan L, Czaplewski DA, Yang X, Gao J. Wavelength-selective Mid-infrared Metamaterial Absorbers with Multiple Tungsten Cross Resonators. *Opt Express* (2018) 26(5):5616–31. doi:10.1364/oe.26.005616
106. Avitzour Y, Urzhumov YA, Shvets G. Wide-angle Infrared Absorber Based on a Negative-index Plasmonic Metamaterial. *Phys Rev B* (2009) 79(4):45131. doi:10.1103/physrevb.79.045131
107. Hao J, Wang J, Liu X, Padilla WJ, Zhou L, Qiu M. High Performance Optical Absorber Based on a Plasmonic Metamaterial. *Appl Phys Lett* (20132010) 96(25):2010.
108. Bossard JA, Lin L, Yun S, Liu L, Werner DH, Mayer TS. Near-Ideal Optical Metamaterial Absorbers with Super-octave Bandwidth. *ACS Nano* (2014) 8(2):1517–24. doi:10.1021/nn4057148
109. Grant J, McCrindle IJH, Cumming DRS. Multi-spectral Materials: Hybridisation of Optical Plasmonic Filters, a Mid Infrared Metamaterial Absorber and a Terahertz Metamaterial Absorber. *Opt Express* (2016) 24(4): 3451–63. doi:10.1364/oe.24.003451
110. Chen N, Hasan D, Pitchappa P, Alioto M, Singh N, Luo X, et al. Polarization-dependent Cut Wire in Mid-infrared Metamaterial Absorber. In: 2017 Conference on Lasers and Electro-Optics Pacific Rim, 2017-Janua. Singapore: CLEO-PR 2017 (2017). p. 1–3. doi:10.1109/cleopr.2017.8118903
111. Desouky M, Mahmoud AM, Swillam MA. Silicon Based Mid-IR Super Absorber Using Hyperbolic Metamaterial. *Sci Rep* (2018) 8(1):2036–15. doi:10.1038/s41598-017-18737-5
112. Ghaderi M, Shahmarvandi EK, Wolffenbuttel RF. CMOS-compatible Mid-IR Metamaterial Absorbers for Out-Of-Band Suppression in Optical MEMS. *Opt Mater Express* (2018) 8(7):1696. doi:10.1364/ome.8.001696
113. Hasan D, Lee C. Hybrid Metamaterial Absorber Platform for Sensing of CO 2 Gas at Mid-IR. *Adv Sci (Weinh)* (2018) 5:17005811–3. doi:10.1002/advs.201700581
114. Ishii S, Uchida K, Dao TD, Wada Y, Saitoh E, Nagao T. Generating Spin Current from Mid Infrared Plasmonic Metamaterial Absorbers. In: 2018 Conference on Lasers and Electro-Optics (CLEO), 12 (2018). p. FF2F. doi:10.1364/cleo_qels.2018.ff2f.88
115. Min P, Song Z, Yang L, Ralchenko VG, Zhu J. Optically Transparent Flexible Broadband Metamaterial Absorber Based on Topology Optimization Design. *Micromachines (Basel)* (2021) 12(11):1419. doi:10.3390/mi12111419
116. Tran MC, Pham VH, Ho TH, Nguyen TT, Do HT, Bui XK, et al. Broadband Microwave Coding Metamaterial Absorbers. *Sci Rep* (2020) 10:1810–1. doi:10.1038/s41598-020-58774-1
117. Amiri M, Tofigh F, Shariati N, Lipman J, Abolhasan M. Review on Metamaterial Perfect Absorbers and Their Applications to IoT. *IEEE Internet Things J* (2021) 8(6):4105–31. doi:10.1109/jiot.2020.3025585
118. Chen H, Yang X, Wu S, Zhang D, Xiao H, Huang K, et al. Flexible and Conformable Broadband Metamaterial Absorber with Wide-Angle and Polarization Stability for Radar Application. *Mater Res Express* (2018) 5(1):15804. doi:10.1088/2053-1591/aaa7ab
119. Cheng YZ, Wang Y, Nie Y, Gong RZ, Xiong X, Wang X. Design, Fabrication and Measurement of a Broadband Polarization-Insensitive Metamaterial Absorber Based on Lumped Elements. *J Appl Phys* (2012) 111(4). doi:10.1063/1.3684553
120. Feng Y. A Frequency and Bandwidth Tunable Metamaterial Absorber in X-Band. *J Appl Phys* (2015) 117(17):173103. doi:10.1063/1.4919753
121. Ghosh S, Bhattacharyya S, Chaurasiya D, Srivastava KV. An Ultrawideband Ultrathin Metamaterial Absorber Based on Circular Split Rings. *Antennas Wirel Propag Lett* (2015) 14(c):1172–5. doi:10.1109/lawp.2015.2396302
122. Shchegolkov DY, Azad AK, O'Hara JF, Simakov EI. Perfect Subwavelength Fishnetlike Metamaterial-Based Film Terahertz Absorbers. *Phys Rev B* (2010) 82(20):205117. doi:10.1103/physrevb.82.205117
123. Xu Z-C, Gao R-M, Ding C-F, Zhang Y-T, Yao J-Q. Multiband Metamaterial Absorber at Terahertz Frequencies. *Chin Phys Lett* (2014) 31(5):54205. doi:10.1088/0256-307x/31/5/054205
124. Wang BX, Zhai X, Wang GZ, Huang WQ. Design of a Four-Band and Polarization-Insensitive Terahertz Metamaterial Absorber Polarization-Insensitive Terahertz. *IEEE Photon J* (2015) 7(1):4600108. doi:10.1109/jphot.2014.2381633
125. Wilbert DS, Hokmabadi MP, Martinez J, Kung P, Kim SM. Terahertz Metamaterials Perfect Absorbers for Sensing and Imaging. *SPIE Proc Ser* (2013) 8585:1–6. doi:10.1117/12.2005709
126. Shen X, Yang Y, Zang Y, Gu J, Han J, Zhang W, et al. Triple-band Terahertz Metamaterial Absorber: Design, experiment, and Physical Interpretation. *Appl Phys Lett* (2012) 101(15):154102. doi:10.1063/1.4757879
127. Su Z, Yin J, Zhao X. Terahertz Dual-Band Metamaterial Absorber Based on graphene/MgF(2) Multilayer Structures. *Opt Express* (2015) 23(2):1679–90. doi:10.1364/OE.23.001679
128. Wang B. Quad-Band Terahertz Metamaterial Absorber Based on the Combining of the Dipole and Quadrupole Resonances of Two SRRs. *IEEE J Selected Top Quan Electron* (2017) 23(4):4700107. doi:10.1109/jstqe.2016.2547325
129. Ben-Xin Wang GZ, Wang BX. Five-Band Terahertz Metamaterial Absorber Based on a Four-Gap Comb Resonator. *J Lightwave Technol* (2015) 33(24): 5151–6. doi:10.1109/jlt.2015.2497740
130. Costa F, Genovesi S, Monorchio A, Manara G. A Circuit-Based Model for the Interpretation of Perfect Metamaterial Absorbers. *IEEE Trans Antennas Propagat* (2013) 61(3):1201–9. doi:10.1109/tap.2012.2227923
131. Wang B-X, Wang L-L, Wang G-Z, Huang W-Q, Li X-F, Zhai X. Metamaterial-Based Low-Conductivity Alloy Perfect Absorber. *J Lightwave Technol* (2014) 32(12):2293–8. doi:10.1109/jlt.2014.2322860
132. Pan W, Yu X, Zhang J, Zeng W. A Broadband Terahertz Metamaterial Absorber Based on Two Circular Split Rings. *IEEE J Quan Electron* (2017) 53(1):2–7. doi:10.1109/jqe.2016.2643279
133. Saadeldin AS, Hameed MFO, Elkaramany EMA, Obayya SSA. Highly Sensitive Terahertz Metamaterial Sensor. *IEEE Sensors J* (2019) 19:7993–9. doi:10.1109/jsen.2019.2918214
134. Lee Y, Kim S-J, Park H, Lee B. Metamaterials and Metasurfaces for Sensor Applications. *Sensors* (2017) 17(8):1726. doi:10.3390/s17081726
135. Ian T, Ang MIW. Highly Sensitive Terahertz Metamaterial Biosensor for Bovine Serum Albumin (BSA) Detection. *Opt Mater Express* (2021) 11(7): 2268–77.
136. Mohanty A, Acharya OP, Appasani B, Mohapatra SK, Khan MS. Design of a Novel Terahertz Metamaterial Absorber for Sensing Applications. *IEEE Sensors J* (2021) 21(20):22688–94. doi:10.1109/jsen.2021.3109158
137. Appasani B. A Hybrid Terahertz Metamaterial Sensor Using a Hexagonal Ring Resonator with Bio-Medical Applications. *Plasmonics* (2021) 1–6.
138. Muntasir M, Sadik F, Islam F. A Review on Plasmonic and Metamaterial Based Biosensing Platforms for Virus Detection. *Sensing Bio-Sensing Res* (2021) 33:100429.
139. Ji W, Zhang Q, Zhang C. High-Performance and Ultra-broadband Metamaterial Absorber Based on Mixed Absorption Mechanisms. *IEEE Access* (2019) 7:57259–66.
140. Yu J, Lang T, Chen H. All-Metal Terahertz Metamaterial Absorber and Refractive Index Sensing Performance. *Photonics* (2021) 17(2):519–24. doi:10.3390/photonics8050164
141. Akgol O, Karaaslan M, Unal E, Sabah C. Implementation of a Perfect Metamaterial Absorber into Multi-Functional Sensor Applications. *Mod Phys Lett B* (2017) 31:1750176. doi:10.1142/s0217984917501767
142. Wu J, Wang P, Huang X, Rao F, Chen X, Shen Z, et al. Design and Validation of Liquid Permittivity Sensor Based on Rcrr Microstrip Metamaterial. *Sensors Actuators A: Phys* (2018) 280:222–7. doi:10.1016/j.sna.2018.07.037
143. Altintas O, Aksoy M, Akgol O, Unal E, Karaaslan M, Sabah C. Fluid, Strain and Rotation Sensing Applications by Using Metamaterial Based Sensor. *J Electrochem Soc* (2017) 164:B567–B573. doi:10.1149/2.1971712jes
144. Xu G, Huang J, Ju Z, Wei Z, Li J, Zhao Q. A Novel Six-Band Polarization-Insensitive Metamaterial Absorber with Four Multiple-Mode Resonators. *Pier C* (2017) 77:133–44. doi:10.2528/pierc17060203

145. Islam M, Rao SJM, Kumar G, Pal BP, Roy Chowdhury D. Role of Resonance Modes on Terahertz Metamaterials Based Thin Film Sensors. *Sci Rep* (2017) 7:7355. doi:10.1038/s41598-017-07720-9
146. Yahiaoui R, Tan S, Cong L, Singh R, Yan F, Zhang W. Multispectral Terahertz Sensing with Highly Flexible Ultrathin Metamaterial Absorber. *J Appl Phys* (2015) 118:083103. doi:10.1063/1.4929449
147. Yahiaoui R, Strikwerda AC, Jepsen PU. Terahertz Plasmonic Structure with Enhanced Sensing Capabilities. *IEEE Sensors J* (2016) 16:2484–8. doi:10.1109/jsen.2016.2521708
148. Ai-Naib I. Biomedical Sensing with Conductively Coupled Terahertz Metamaterial Resonators. *IEEE J Sel Top Quan Electron.* (2017) 23: 4700405.
149. Xie Q, Dong G-X, Wang B-X, Huang W-Q. High-Q Fano Resonance in Terahertz Frequency Based on an Asymmetric Metamaterial Resonator. *Nanoscale Res Lett* (2018) 13:294. doi:10.1186/s11671-018-2677-0

Conflict of Interest: The authors declare that the research was conducted in the absence of any commercial or financial relationships that could be construed as a potential conflict of interest.